PRECIPITATION DOWNSCALING: METHODOLOGIES AND HYDROLOGIC APPLICATIONS

Efi Foufoula-Georgiou

St. Anthony Falls Laboratory
Dept. of Civil Engineering
University of Minnesota

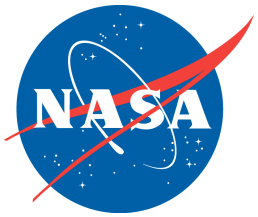

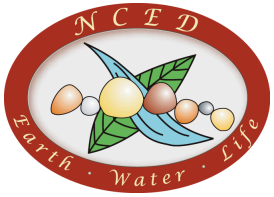

Going up and down the scales…

- The scales involved in GPM are unprecedented (microphysical to global scale)
- There is no hope to explicitly resolve all scales everywhere. Discrepancies between: process scale, observational scale and modeling scale
- Small scales matter in getting the larger scales right (NL interactions that grow over time)
- Upscaling = Find closures or parameterizations that "summarize" the effect of small scales without explicitly resolving them, e.g, convective parameterizations
- Downscaling = Statistical "reconstruction" of the missing variability at sub-grid scales, i.e., at scales smaller than the satellite footprint or the model "resolution scale".

Lessons learned the hard way…

- There is no way to do proper upscaling or downscaling without an exhaustive study of how the process variability changes over scales: from the smallest to the largest scale

- The “numerical laboratory” of Greg Tripoli is an example for redoing the upscaling of microphysics

- The extensive atmospheric BL turbulence field campaigns are examples for coming up with better ABL parameterizations

- *Understanding the multiscale statistical structure of rainfall is a prerequisite for developing precipitation downscaling schemes, techniques for merging observations at different scales, or for comparing model outputs to observations at different scales (model verification)*

Spatial Variability and Intermittency are Functions of Scale

Scale (pixel size):

2x2 km

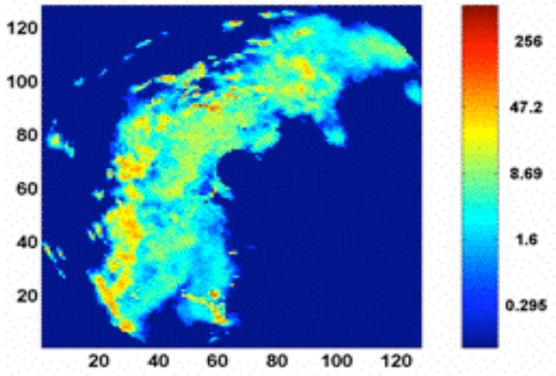

8x8 km

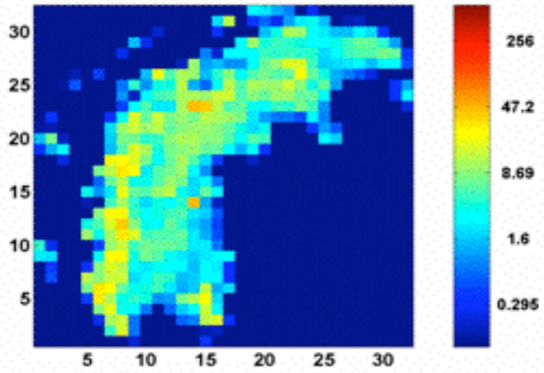

32x32 km

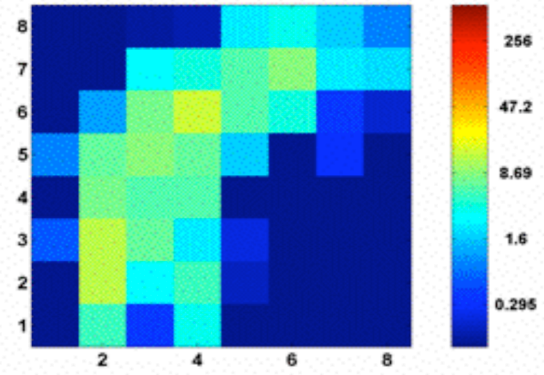

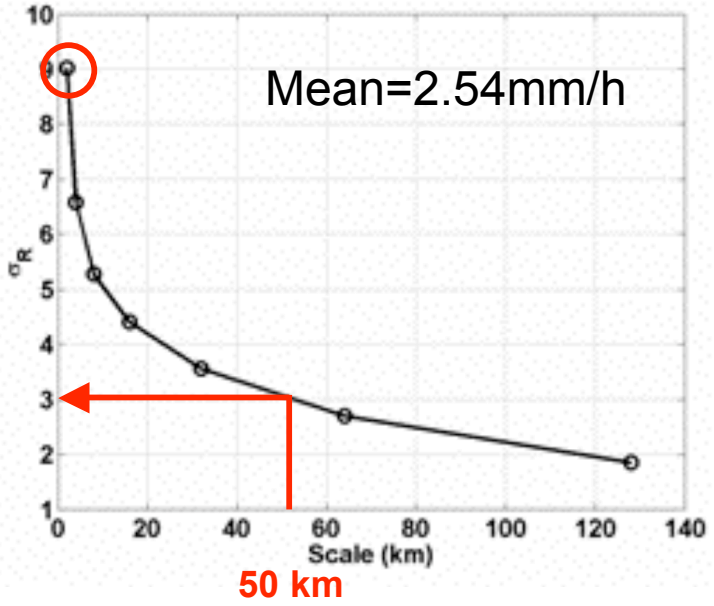

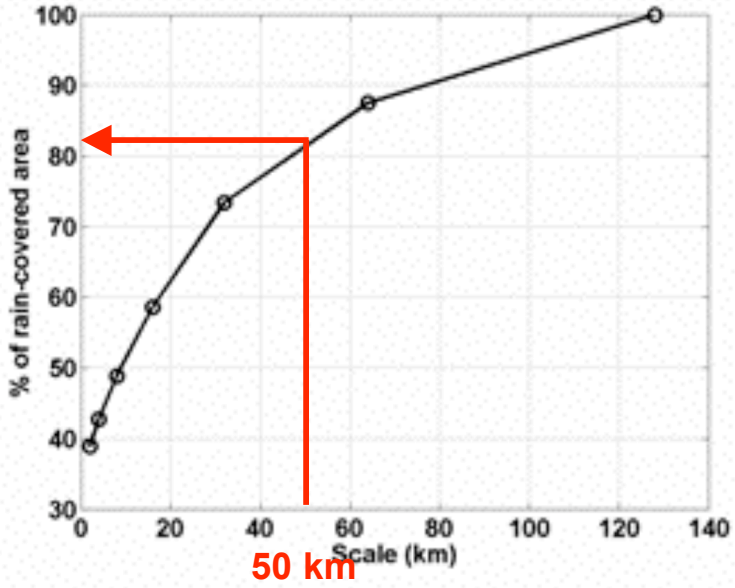

➢ Having same variability at a large scale does **not** imply same variability at smaller scales

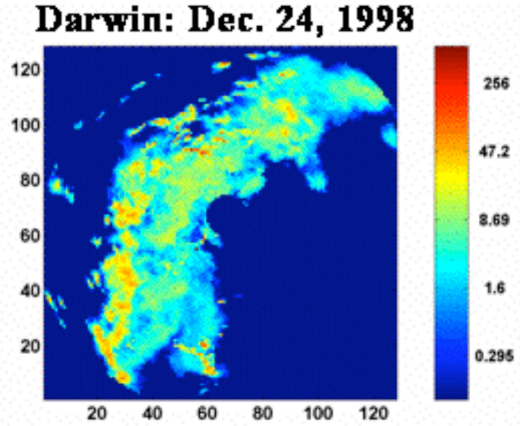

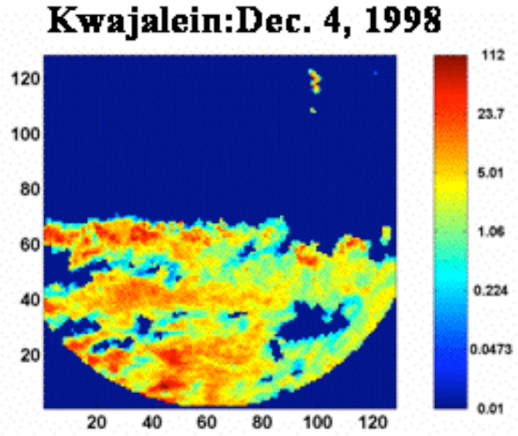

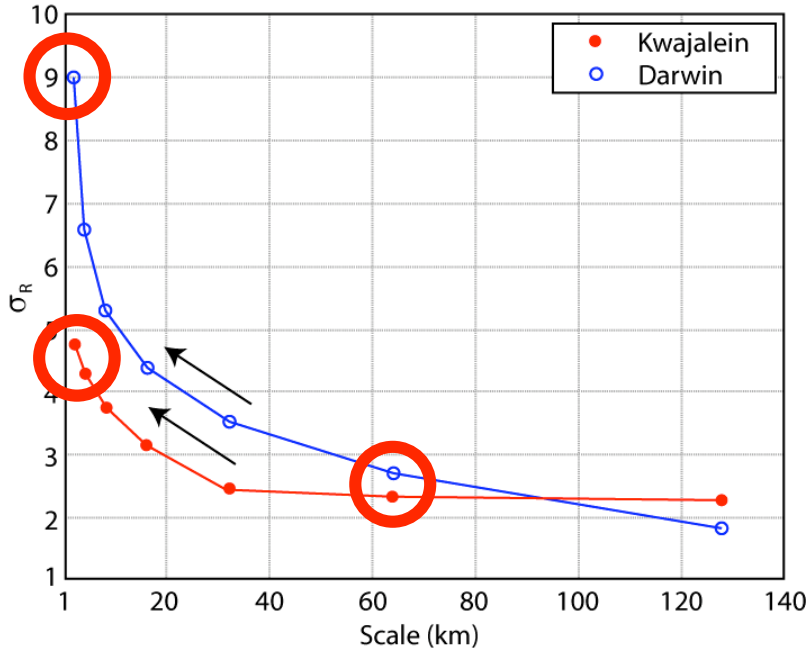

- How can we reconstruct unobserved variability?
- What exogenous parameters might help?

Premises of Statistical Downscaling

- There is a substantial evidence to suggest that despite the very complex patterns of precipitation, there is an underlying simpler structure which exhibits scale-invariant statistical characteristics

- If this scale invariance is unraveled and quantified, it can form the basis of moving up and down the scales: important for efficient and parsimonious downscaling methodologies

Outline of Talk

1. Multi-scale analysis of spatial precipitation
2. Relation of statistical parameters to physical observables
3. A spatial downscaling scheme
4. A space-time downscaling scheme
5. Merging multiscale/multisensor observations
6. Hydrologic applications: beyond hydrographs!

Multiscale Analysis – 1D example

$$\{x_1, x_2, x_3, x_4, x_5, x_6, x_7, x_8\}$$

$$\underbrace{\frac{x_1 + x_2}{2} \quad \frac{x_3 + x_4}{2} \quad \frac{x_5 + x_6}{2} \quad \frac{x_7 + x_8}{2}}_{\bar{X}_1}$$

$$\underbrace{\frac{x_1 + x_2 + x_3 + x_4}{4} \quad \frac{x_5 + x_6 + x_7 + x_8}{4}}_{\bar{X}_2}$$

$$\underbrace{\frac{x_1 + x_2 + x_3 + x_4 + x_5 + x_6 + x_7 + x_8}{8}}_{\bar{X}_3}$$

Multiscale Analysis – 1D example

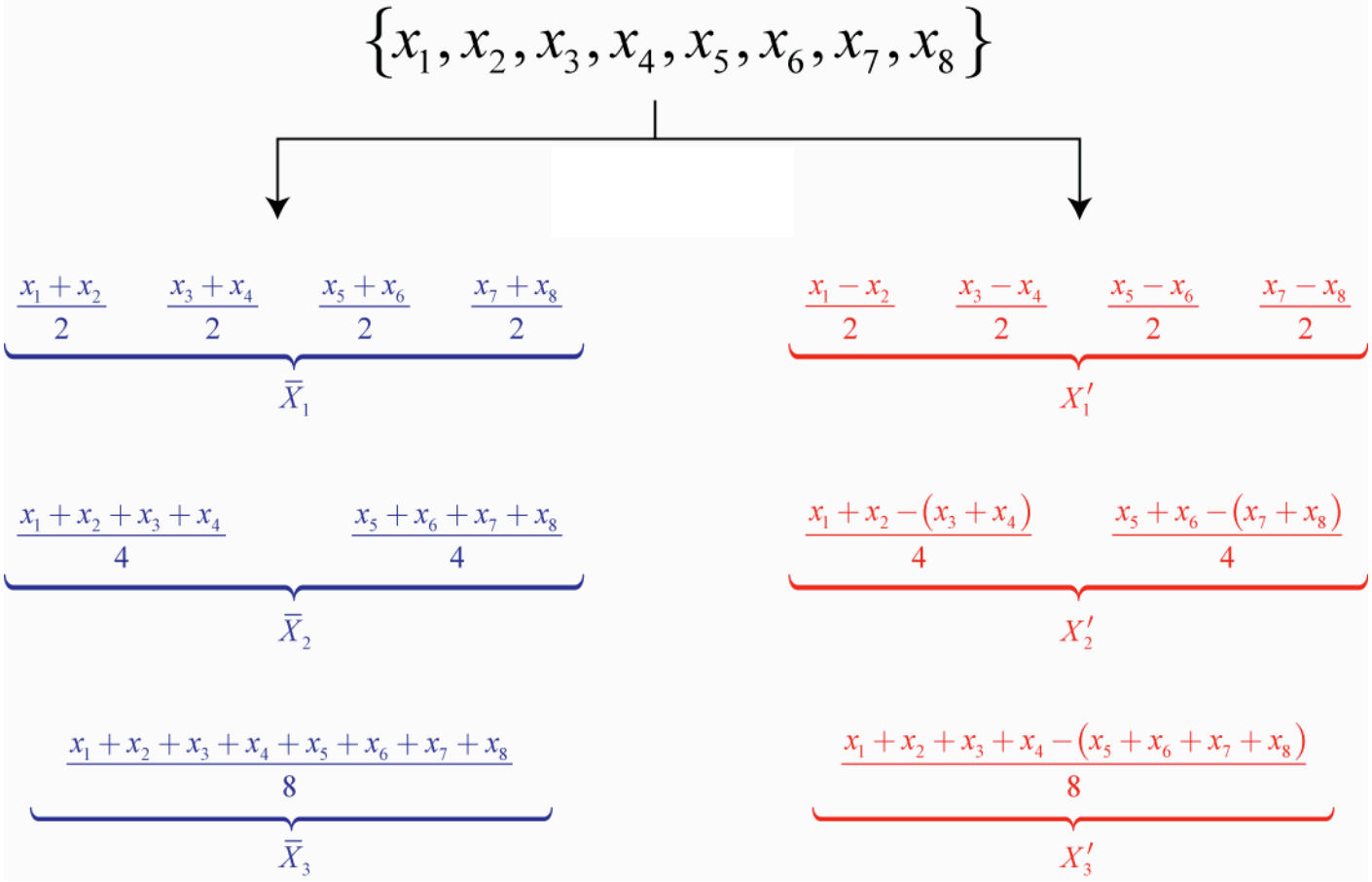

Multiscale Analysis – 1D example

$$\{x_1, x_2, x_3, x_4, x_5, x_6, x_7, x_8\}$$

$$\underbrace{\frac{x_1+x_2}{2} \quad \frac{x_3+x_4}{2} \quad \frac{x_5+x_6}{2} \quad \frac{x_7+x_8}{2}}_{\bar{X}_1} \qquad \underbrace{\frac{x_1-x_2}{2} \quad \frac{x_3-x_4}{2} \quad \frac{x_5-x_6}{2} \quad \frac{x_7-x_8}{2}}_{X'_1}$$

$$\underbrace{\frac{x_1+x_2+x_3+x_4}{4} \quad \frac{x_5+x_6+x_7+x_8}{4}}_{\bar{X}_2} \qquad \underbrace{\frac{x_1+x_2-(x_3+x_4)}{4} \quad \frac{x_5+x_6-(x_7+x_8)}{4}}_{X'_2}$$

$$\underbrace{\frac{x_1+x_2+x_3+x_4+x_5+x_6+x_7+x_8}{8}}_{\bar{X}_3} \qquad \underbrace{\frac{x_1+x_2+x_3+x_4-(x_5+x_6+x_7+x_8)}{8}}_{X'_3}$$

Haar Wavelet Multiscale Filter:

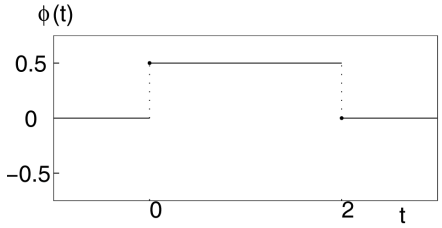

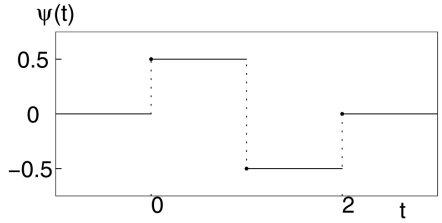

2D Multiscale Rainfall Analysis

• Local gradients of rainfall depend on local average rainfall intensities

•However, local standardized gradients

- Are approximately independent of local averages
- Obey approximately a Normal distribution centered around zero, i.e., have only 1 parameter to worry about in each direction
- Their variance varies log-log linearly with scale

A storm-dependent parameter

Variance at known large scale

(See Perica and Foufoula-Georgiou, JGR, 1996)

Relation of statistical parameter H to physical observables

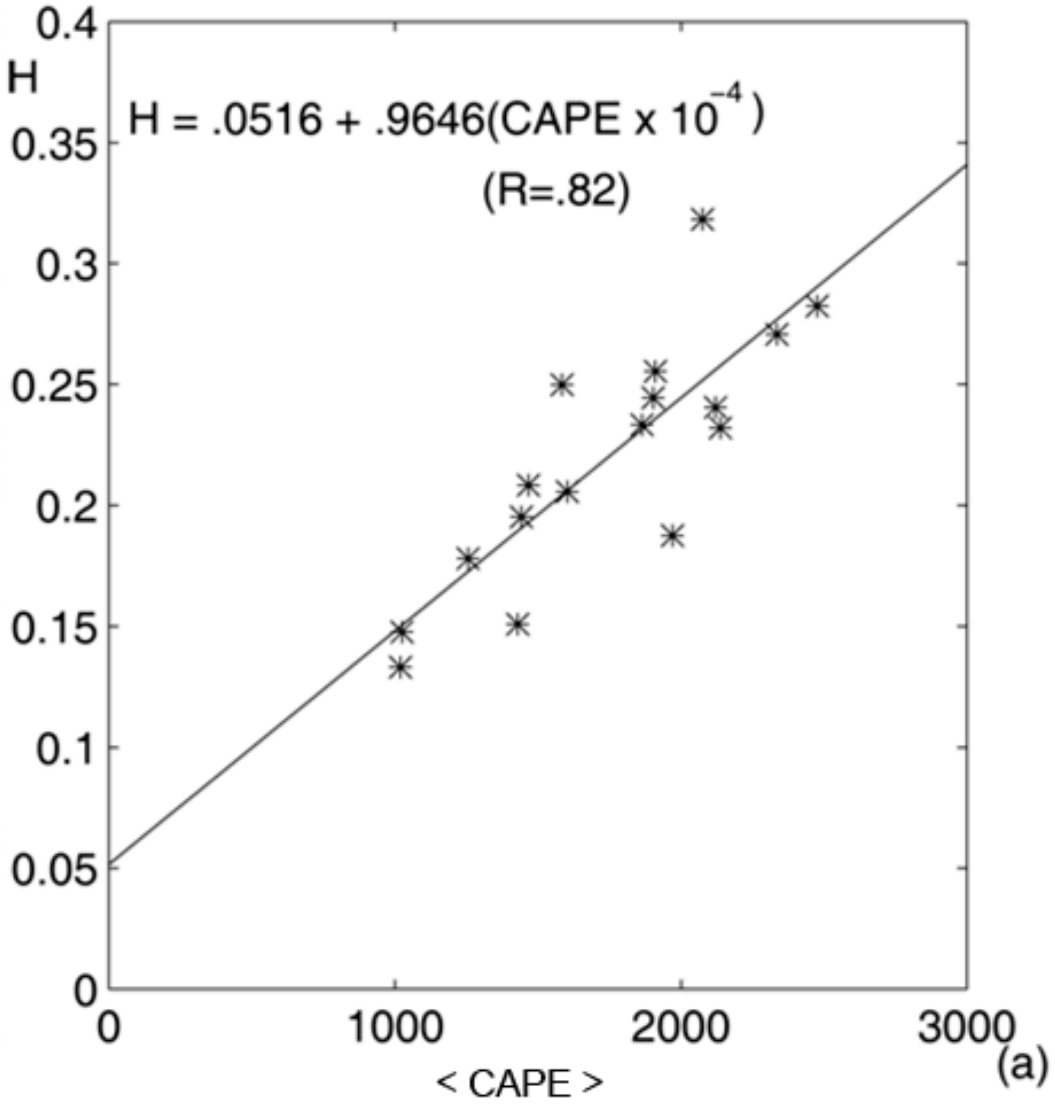

θ_c = potential *T* of an air parcel lifted from the surface to the level *z*

θ_{env} = potential *T* of the unsaturated environment at the same level

LFC = level of free convection

EL = Equilibrium level

CAPE (m^2/s^2) is a measure of potential instability

<CAPE> = representative CAPE

(See Zhang and Foufoula-Georgiou, JGR, 1997)

Examples of Downscaling

64x64 km

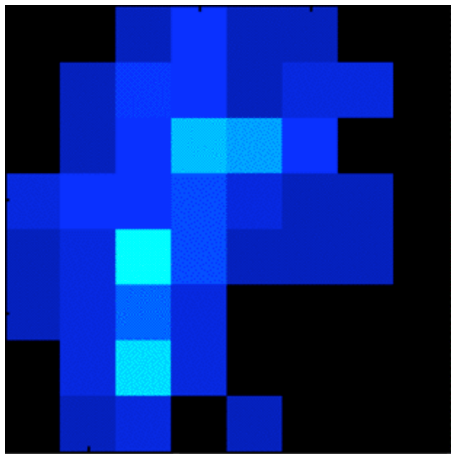

4x4 km

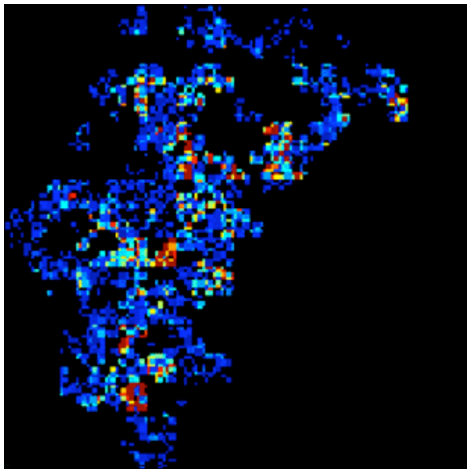

Downscaled

4x4 km

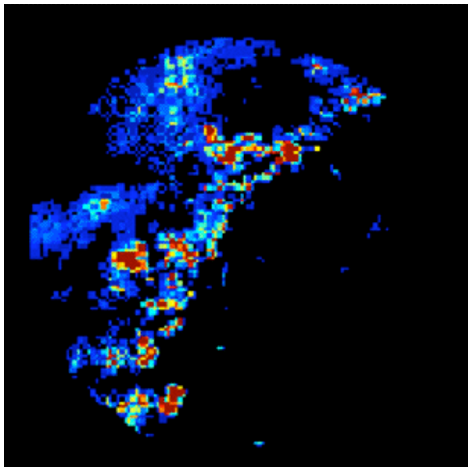

Observed

Given:

-Large scale means (e.g., 64x64 km average rain)

-Pre-storm environmental conditions (CAPE)

-Parameters of predictive equations (CAPE → H, C)

Provide (via statistical downscaling based on IWT):

Rainfall at any smaller scale

IWT – Inverse Wavelet Transform

(See Perica and Foufoula-Georgiou, JGR, 1996)

Examples of Downscaling

64x64 km

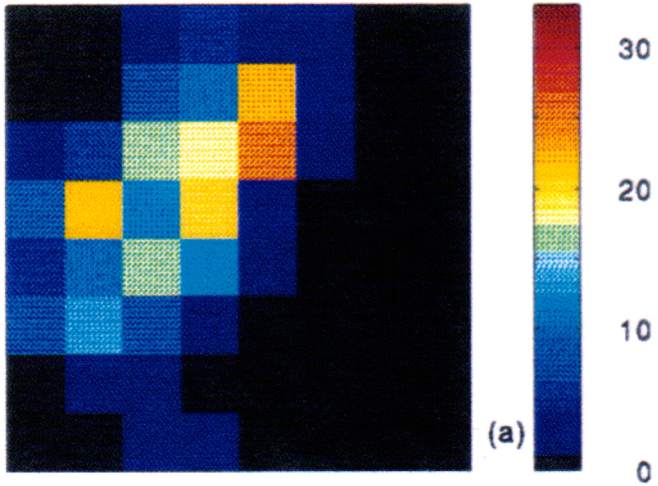

4x4 km

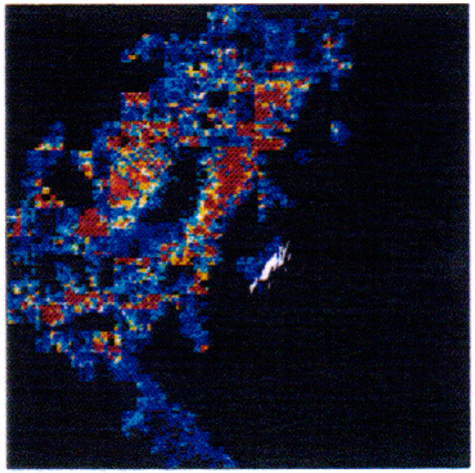

Downscaled

4x4 km

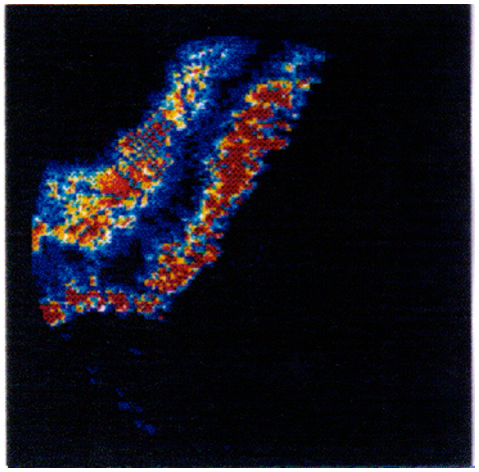

Observed

(See Perica and Foufoula-Georgiou, JGR, 1996)

Space-Time Downscaling

Spatial variability changes over time . . .

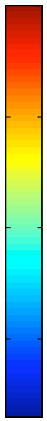

t = 1 hr

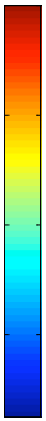

t = 2 hr

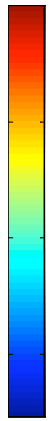

t = 3 hr

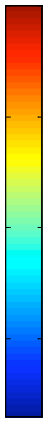

t = 4 hr

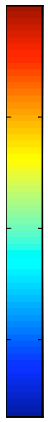

t = 5 hr

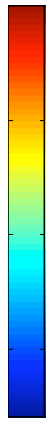

t = 6 hr

January 27th, 1992 Darwin, Hourly Accumulation

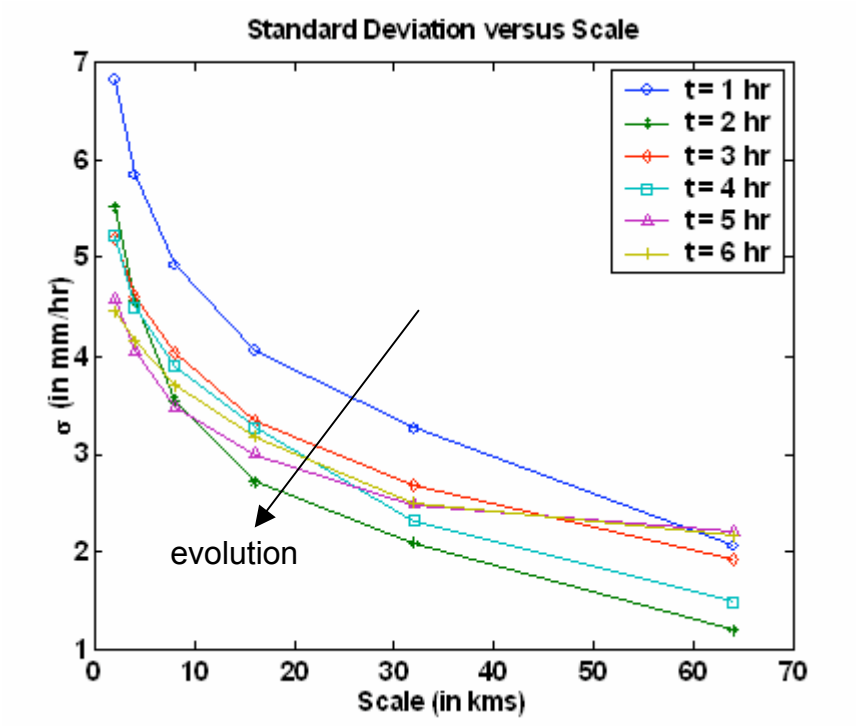
Standard Deviation versus Scale
σ (in mm/hr)
Scale (in kms)
t = 1 hr
t = 2 hr
t = 3 hr
t = 4 hr
t = 5 hr
t = 6 hr
evolution

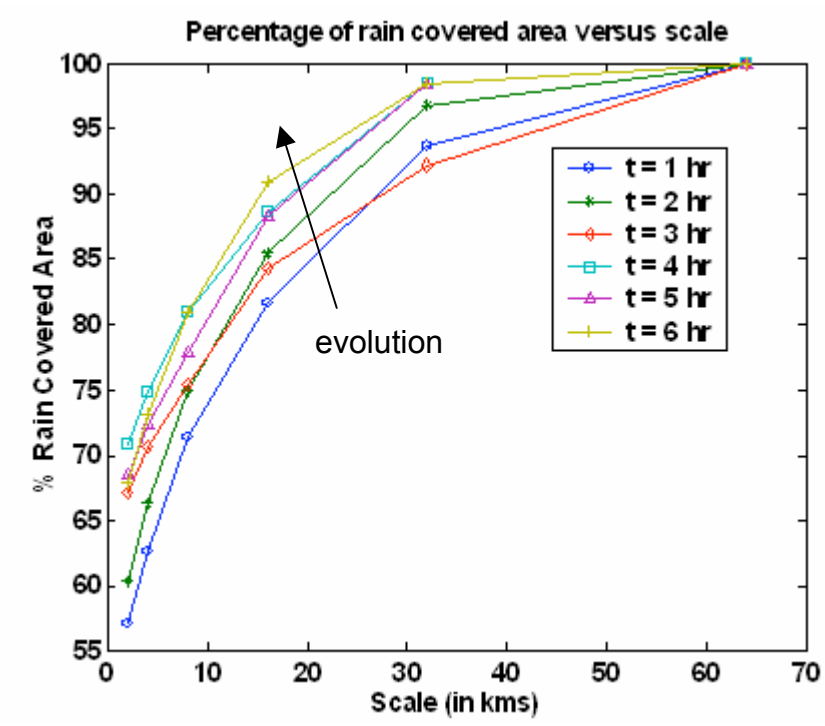
Percentage of rain covered area versus scale
% Rain Covered Area
Scale (in kms)
t = 1 hr
t = 2 hr
t = 3 hr
t = 4 hr
t = 5 hr
t = 6 hr
evolution

Statistical Evolution of Rainfall: PDFs of Δln*I*

Pixel Size: Δx=2 km

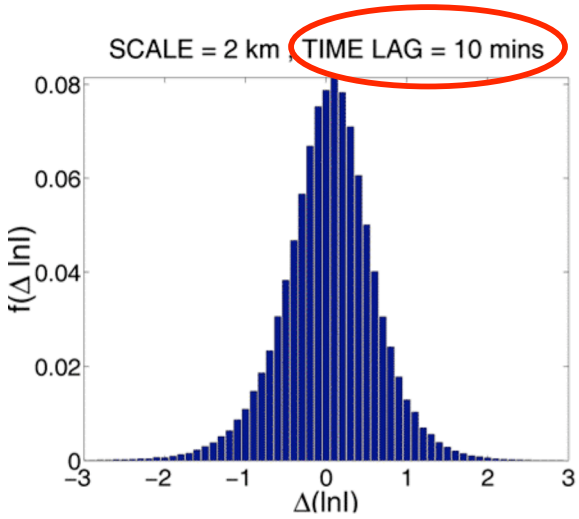

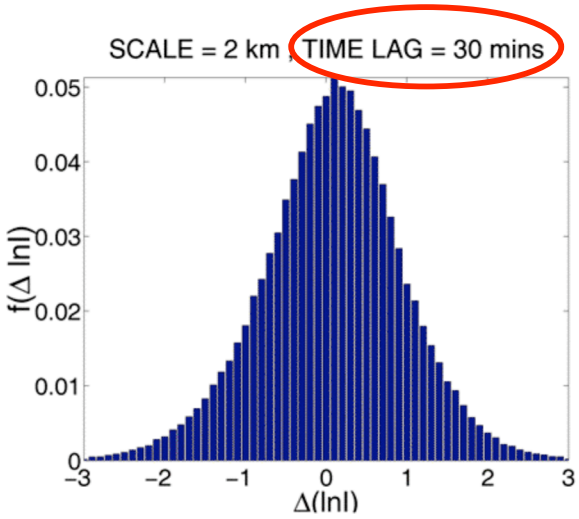

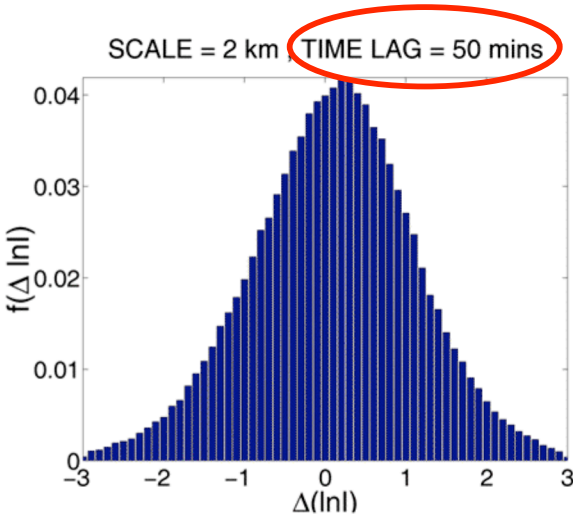

Pixel Size: Δx=8 km

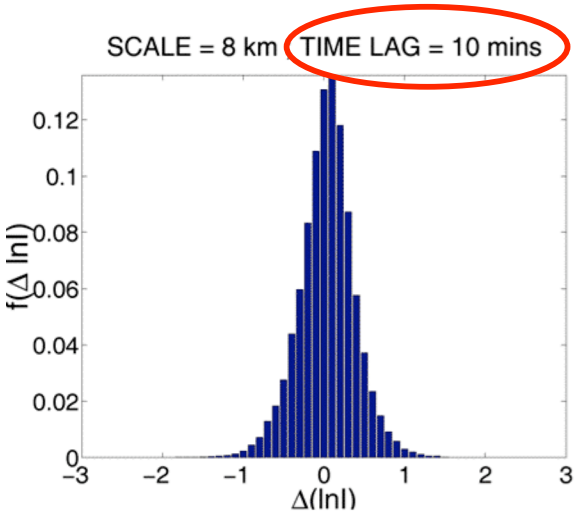

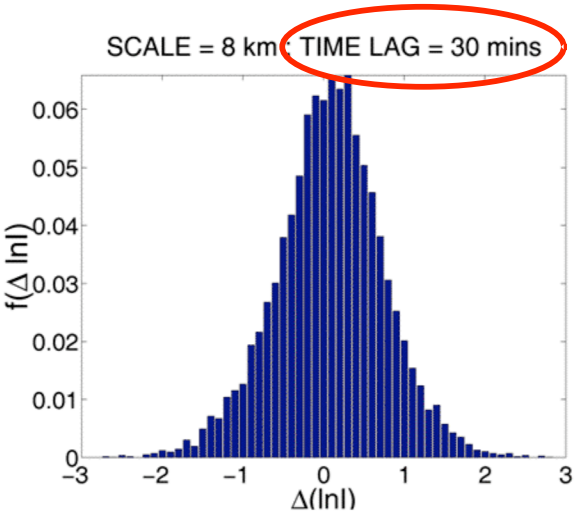

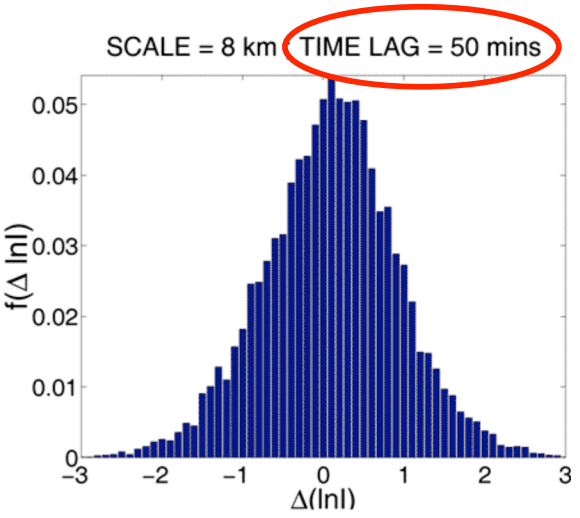

Question: Is it possible to rescale space and time such that some scale-invariance is unraveled?

- Look for transformation that relate the dimensionless quantities (/ and (/
- Possible only via transformation of the form : "Dynamic scaling"

(See Venugopal, Foufoula-Georgiou and Sapozhnikov, JGR, 1999)

Iso-PDFs

σ (_lnI) = 0.6; z = 0.58

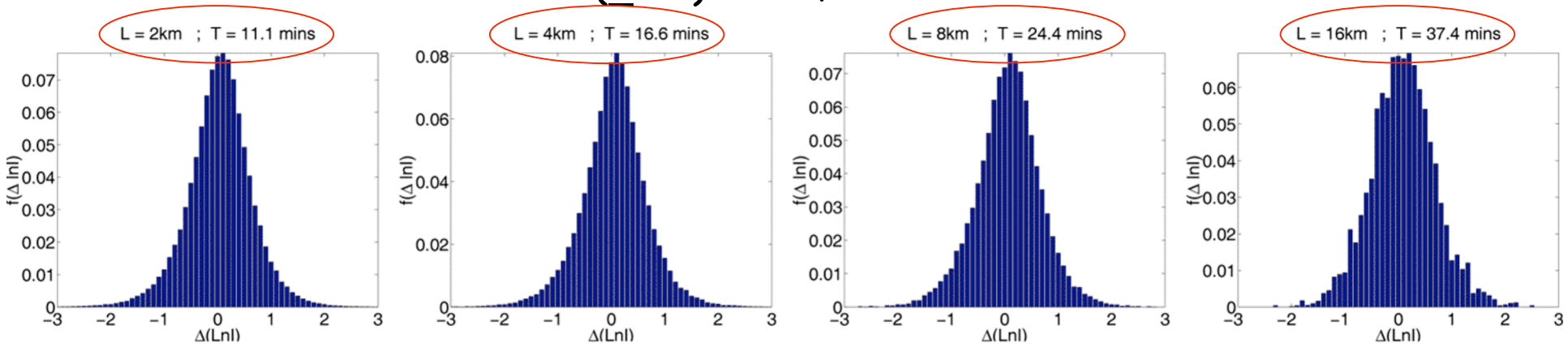

σ (_lnI) = 0.8; z = 0.51

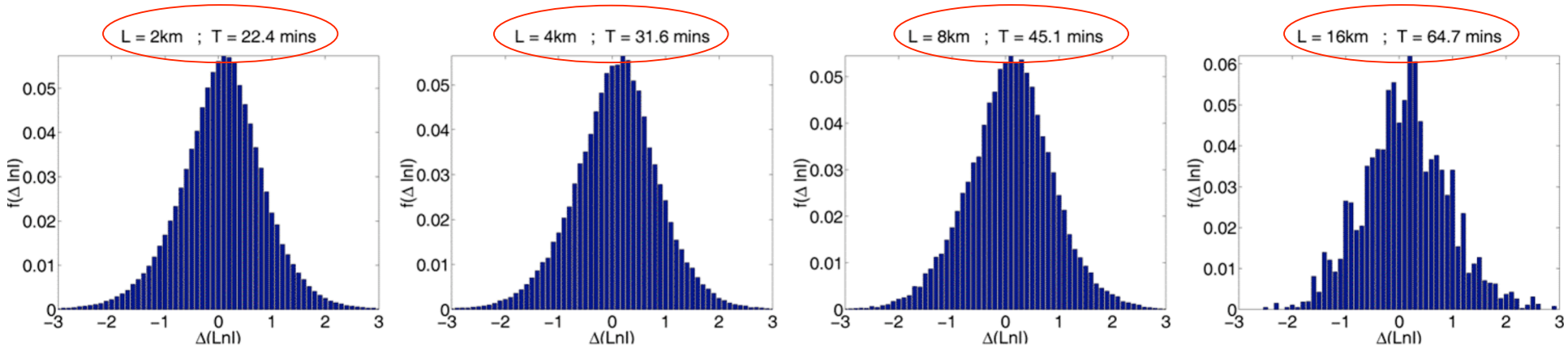

Space-time downscaling preserves temporal persistence

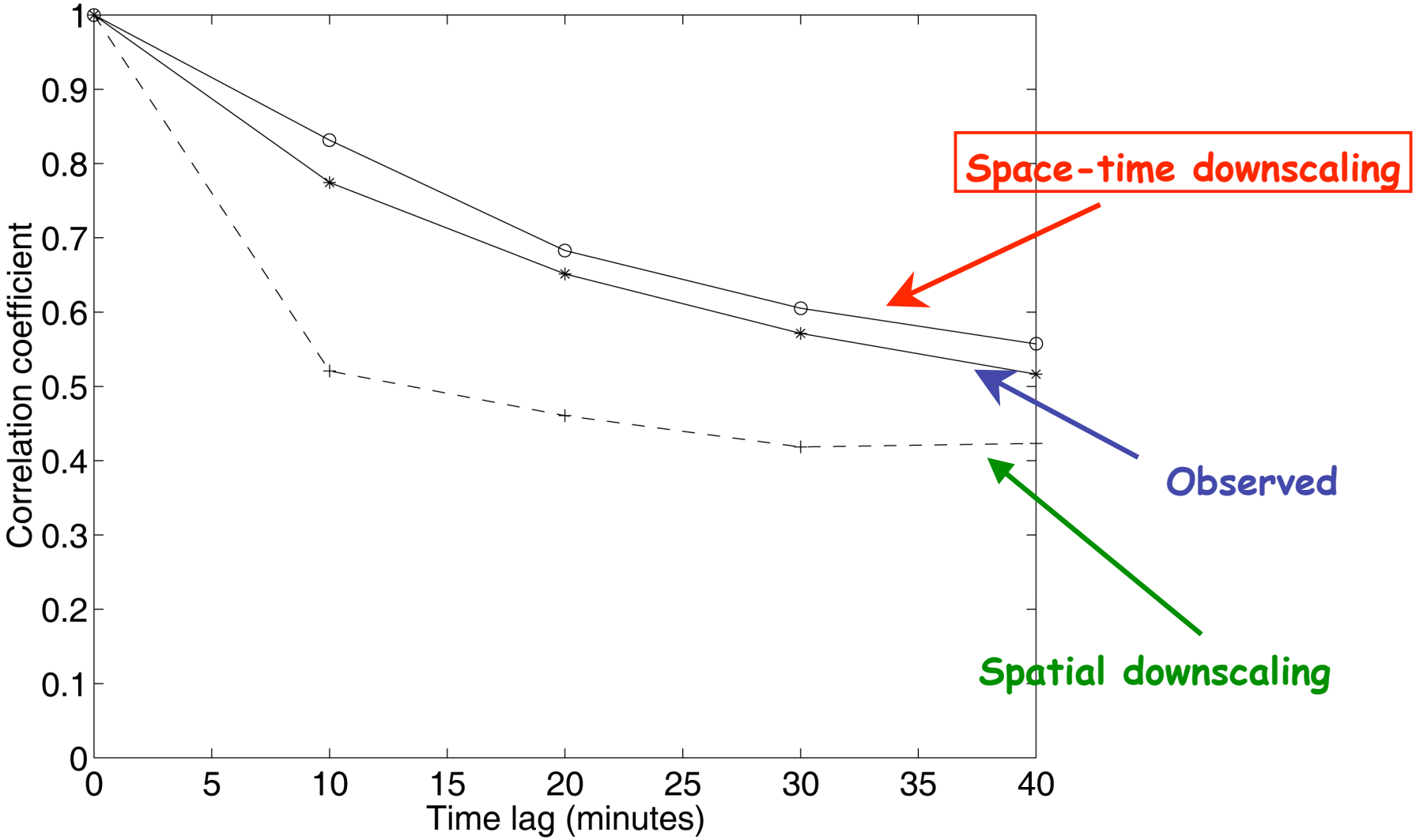

Downscaling Precipitation for Improving Surface Energy Fluxes

- Ignoring subgrid-scale rainfall variability has been found to affect prediction accuracy of water and energy fluxes at grid scales (due to small-scale NL interactions which amplify).
- Example: Modeling the effects of the July 4-5, 1995 storm over Midwestern US

R12: Run coupled MM5-BATS; at 12km resolution

R3: Downscale rainfall at 3 km → run BATS at 3 km → couple to MM5 @ 12 km.

R3-12: "error" due to ignoring subgrid-scale rainfall 32 hours later.

Error R3-R12:

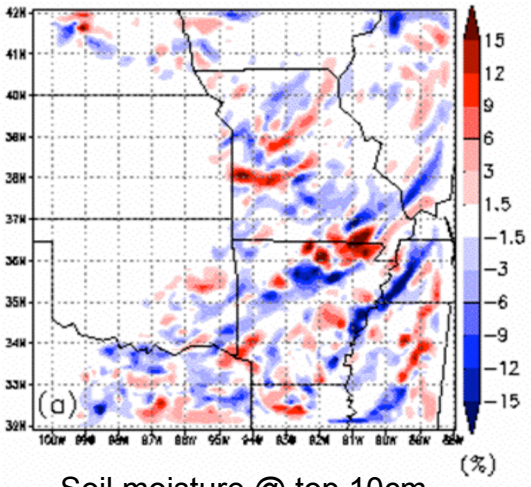

Soil moisture @ top 10cm

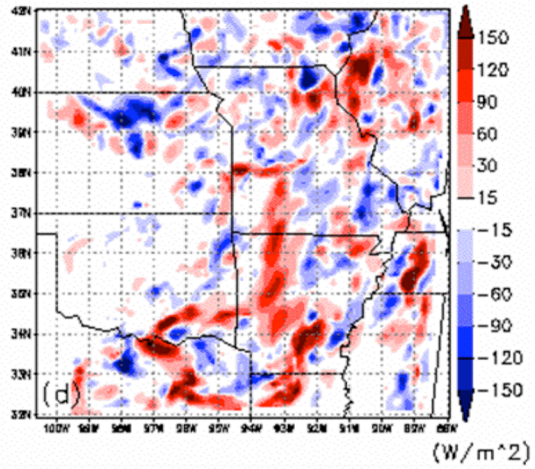

Latent heat flux from surface

Result:

- Notice that the 3 km rainfall heterogeneities going through the coupled land-atmosphere system propagate to larger scale (approx. 40 km) anomalies in water and energy fluxes as seen in these figures.

(See Nykanen, Foufoula-Georgiou, and Lapenta, J. Hydrometeorology, 2001)

Downscaling hydrometeors for improving CRM composition

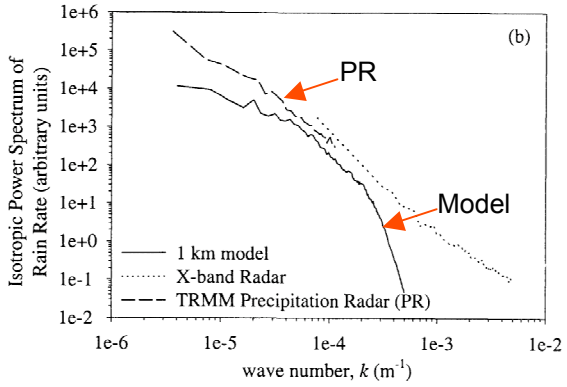

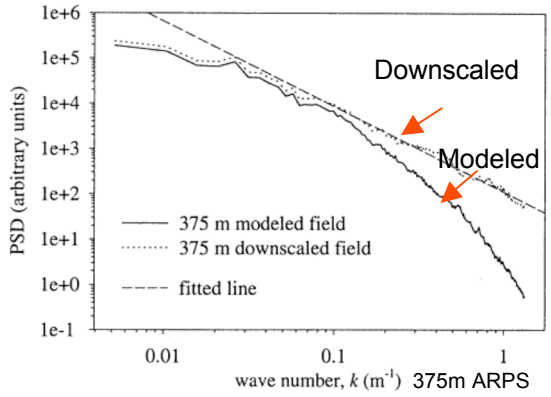

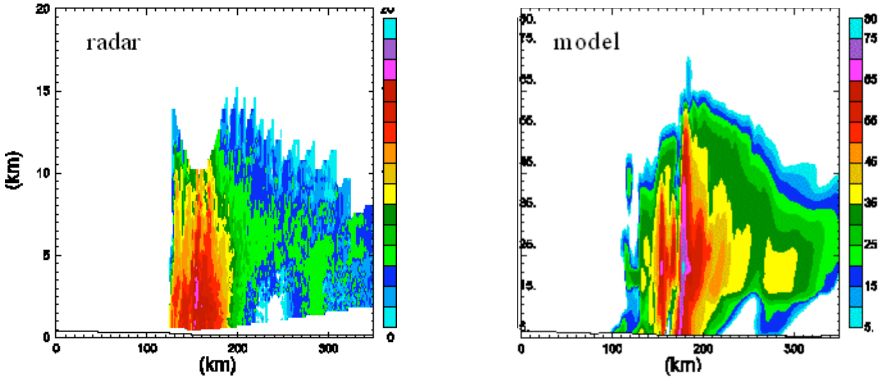

- CRMs at 1-2 km resolution underestimate the hydrometeor variability and do not faithfully reproduce the storm vertical structure
- Can re-introduce this subgrid scale variability via hydrometeor downscaling
- Can use to improve the scattering properties of cloud data bases used in rainfall retrieval

(See: Harris, Foufoula-Georgiou, Kummerow, JGR, 2003; Smedsmo, Venugopal, Foufoula-Georgiou, Droegemeier, and Kong, JAM, 2005)

Challenges in Precipitation Downscaling for GPM

1. Multiscale statistics of rainfall vary geographically and seasonally. Current parameterizations are in terms of CAPE but more refined and robust storm-specific predictive equations for downscaling are needed over diverse storm environments.

2. The parameters controlling the temporal evolution of subgrid-scale statistics (for space-time downscaling) have not yet been related to physical attributes of the storm. Since preserving the short-term (within 3 hours) temporal persistence of downscaled rainfall is important for many applications, more research is needed on this topic.

3. Schemes for downscaling orographic precipitation need to be developed. They should not be purely statistical but take advantage of the underlying orography in a hybrid physical-statistical framework.

Merging Multisensor/Multiscale Observations

- Optimal estimation at a desired scale, given partial or noisy measurements at different scales
- Introduced a multi-scale Kalman-Filtering methodology (SRE=scale-recursive estimation) and demonstrated its performance

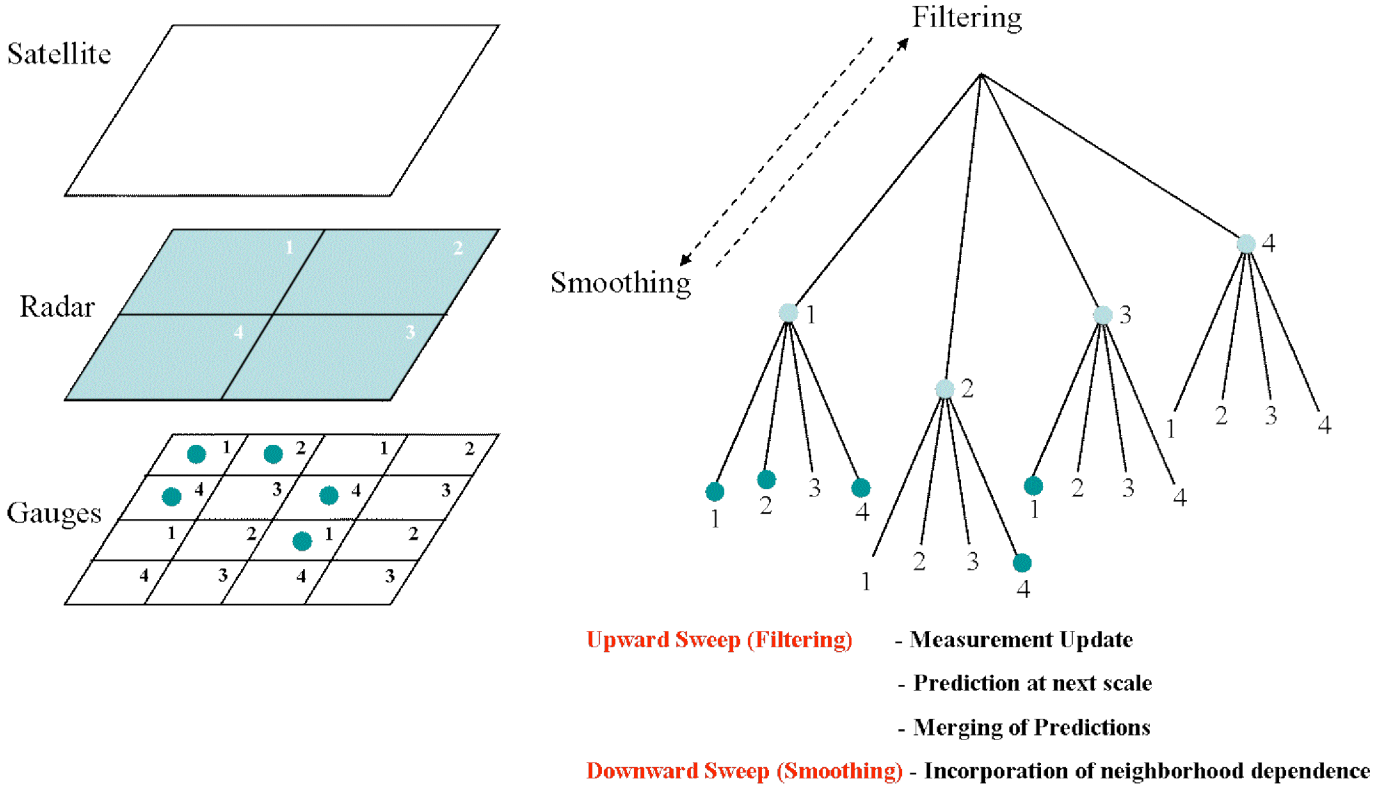

(See: Tustison, Harris and Foufoula-Georgiou, JGR, 2001; Gupta, Venugopal and Foufoula-Georgiou, JGR, 2006)

GPM and Hydrology: Much Beyond Hydrograph Prediction

Rainfall is the driver…

•Predicting the water, sediment and nutrient cycling and the ecosystem response to natural or anthropogenic stresses has become imperative.

•High resolution topography is becoming readily available around the world and in remote mountainous areas.

•Our understanding of how the physical template (river network topology, geomorphic features) affects ecosystem dynamics (vegetation, food webs, stream water quality) increases rapidly.

• Wireless technology and new environmental sensors and laboratory to field-scale experiments, adds to this understanding.

GPM Opportunity: Debris Flow and Landsliding

(Highest debris flows: highest rainfall over steep areas)

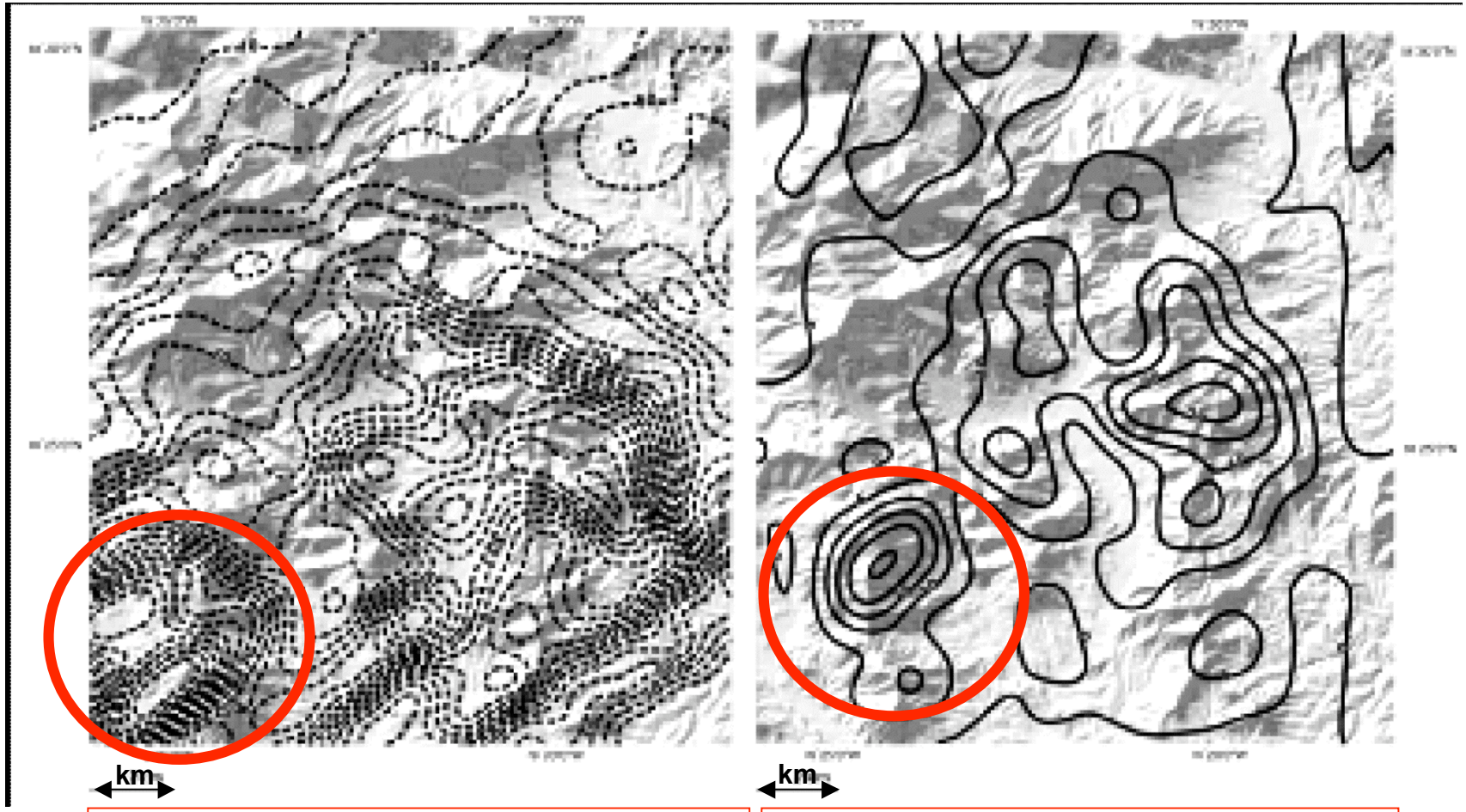

Maximum hourly rainfall contours from NEXRAD

Contours of debris-flow concentration

June 27, 1995 Rapidan Storm, Madison County

(See Wieczorek et al., 1993)

GPM and Probabilistic Risk Assessment

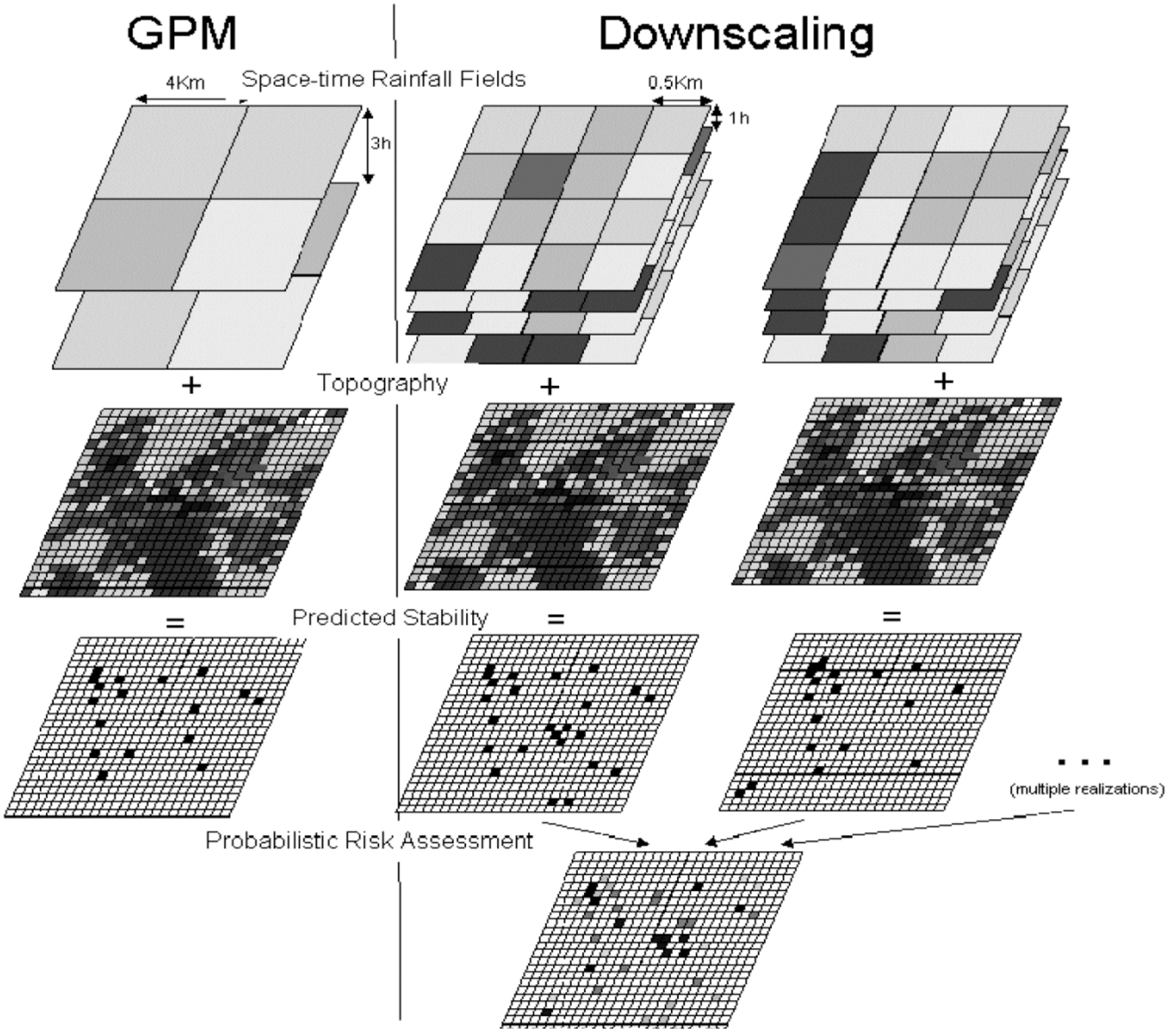

GPM opportunity: Sediment delivery to the streams

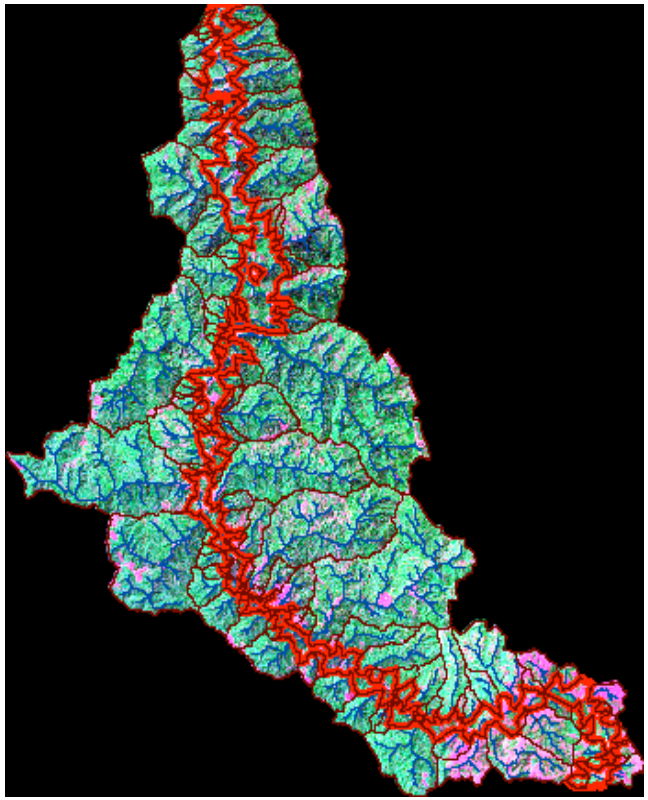

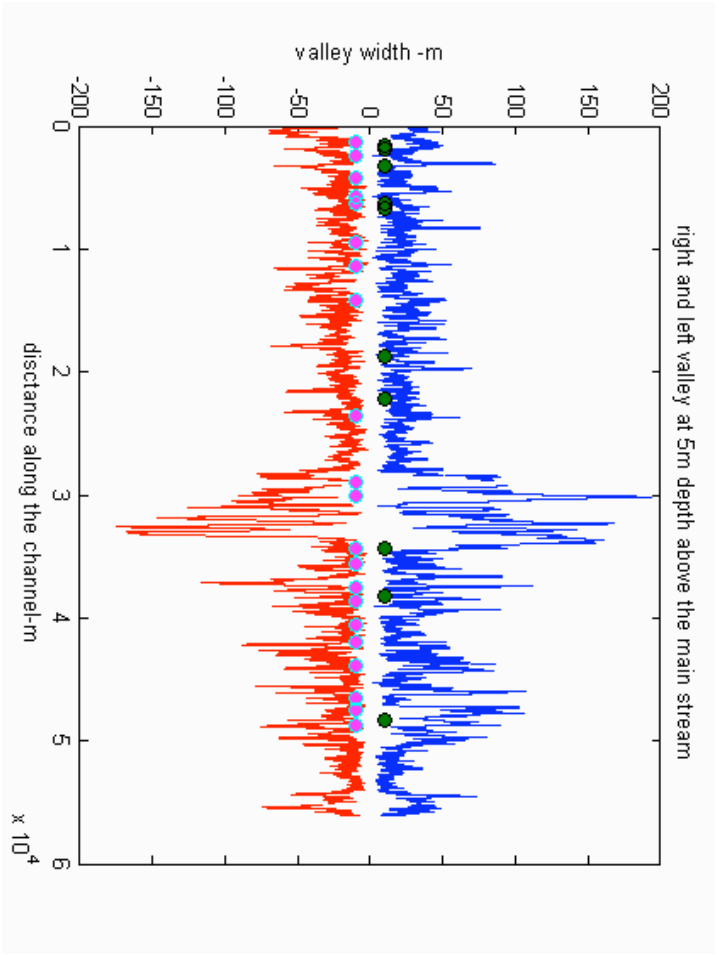

Sklar, Dietrich, Foufoula-Georgiou, Lashermes,Bellugi, WRR, 2006

Gangodagamage and Foufoula-Georgiou, 2006

GPM Opportunity: Biological and Ecological Response

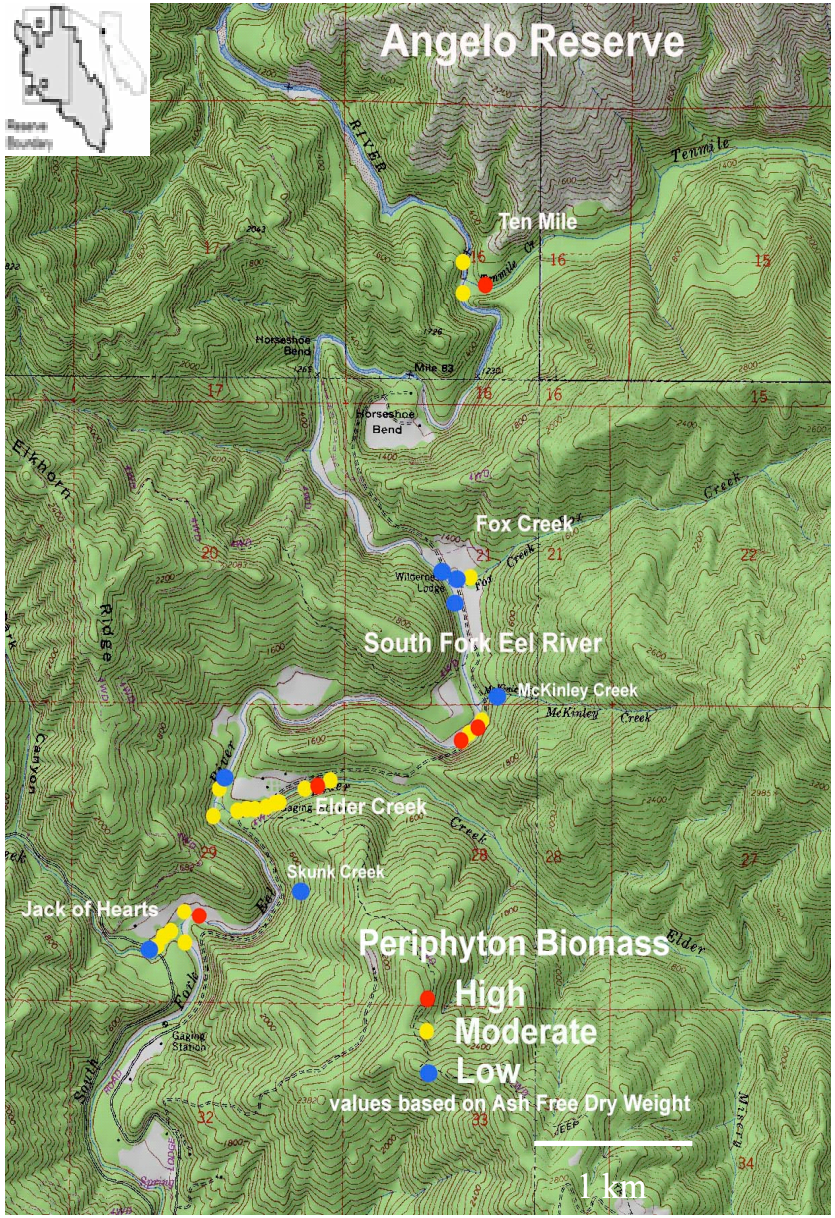

- Precipitation affects the composition of hillslope sediment entering the streams
- Excessive loading of fine sediment smothers bed topography and reduces growth and survival of juvenile steelhead (the most serious impairment of many western US Rivers)
- Benthic insects hidden in embedded sediments are less available to fish
- The whole food web is affected

Research at NCED (National Center for Earth-surface Dynamics)

A Field Site to Advance Understanding of Coupled Processes

Angelo Coast Range Reserve (ACRR) in the Eel River Basin

Micro-scale to field-scale Experiments

Rainfall

⇕

vegetation

⇕

biotic process

⇕

channel morphology

GPM offers unique opportunities for the Earth Sciences . . .

1. High resolution topography becomes readily available around the world and in remote mountainous areas.

   GPM offers the potential for understanding and predicting:
   - Rainfall-induced hazards
   - Ecosystem response to extremes or altered climates
   - System recovery after disruption

2. Should not miss the conceptual opportunity offered by GPM of substituting space for time; unprecedented chance to study diverse environments simultaneously to speed up understanding and predictive ability. Needs a methodic framework of study.
   - Also offers the ability for Probabilistic Risk Assessment

3. Even at resolution of 4 km, 3 hr over the globe the opportunities are tremendous.

4. Precipitation downscaling (<4 km in space, <3 hours in time) is imperative for some applications and despite progress several challenges still exist.

Precipitation at the Center of Geosciences?

sors represents an additional dimension of sensitivity and specificity for molecular imaging. The depletion process generating the image contrast depends on several parameters, including saturation power and time, sensor concentration, and ambient temperature. The latter parameter provides another promising approach to increase sensitivity even further, because the exchange rate increases considerably when approaching 37°C (*10*). Characterization of the saturation dynamics is currently under way and will reveal optimized parameters for future applications.

The technique is also quite promising for biomedical imaging in vivo. A typical surface coil of 20 cm diameter detects a volume of ca. 2.1 liters, thus decreasing S/N for a (2.8 mm)^3 voxel by a factor of 27.2 compared with our setup. This loss is less than 50% of the gain for an optimized system using >45% polarized isotopically enriched ^{129}Xe. An isotropic resolution of 2 to 3 mm is feasible without signal averaging for a concentration of pure polarized ^{129}Xe that is ~2 μM in tissue. This minimum value is below those observed for direct injection of Xe-carrying lipid solutions into rat muscle (70 μM) or for inhalation delivery for brain tissue (8 μM) used in previous studies that demonstrated Xe tissue imaging in vivo (*17*). Sensitive molecular imaging of the biosensor is therefore possible as long as the distribution of dissolved xenon can be imaged with sufficient S/N and the biosensor target is not too dilute, because HYPER-CEST is based on the detection of the free Xe resonance, not direct detection of the biosensor resonance.

The HYPER-CEST technique is amenable to any type of MRI image acquisition methodology. We demonstrated CSI here, but faster acquisition techniques that incorporate a frequency encoding domain such as FLASH (fast low angle shot) have been successfully used to acquire in vivo Xe tissue images (*17*).

The modular setup of the biosensor (i.e., the nuclei that are detected are not covalently bound to the targeting molecule) allows accumulation of the biosensor in the tissue for minutes to hours before delivery of the hyperpolarized xenon nuclei, which have much higher diffusivity. In combination with the long spin-lattice relaxation time of Xe, this two-step process optimally preserves the hyperpolarization before signal acquisition. Biosensor cages that yield distinct xenon frequencies allow for multiplexing to detect simultaneously several different targets (*18*). Also the serum- and tissue-specific Xe NMR signals (*19*, *20*) arising after injection of the carrier medium can be used for perfusion studies (Fig. 3B) in living tissue, making Xe-CSI a multimodal imaging technique.

References and Notes

1. J. M. Tyszka, S. E. Fraser, R. E. Jacobs, *Curr. Opin. Biotechnol.* **16**, 93 (2005).
2. A. Y. Louie *et al.*, *Nat. Biotechnol.* **18**, 321 (2000).
3. S. Aime, C. Carrera, D. Delli Castelli, S. Geninatti, E. Terreno, *Angew. Chem. Int. Ed.* **44**, 1813 (2005).
4. M. S. Albert *et al.*, *Nature* **370**, 199 (1994).
5. M. M. Spence *et al.*, *Proc. Natl. Acad. Sci. U.S.A.* **98**, 10654 (2001).
6. T. J. Lowery *et al.*, *Magn. Reson. Imaging* **21**, 1235 (2003).
7. K. Bartik, M. Luhmer, J. P. Dutasta, A. Collet, J. Reisse, *J. Am. Chem. Soc.* **120**, 784 (1998).
8. C. Hilty, T. J. Lowery, D. E. Wemmer, A. Pines, *Angew. Chem. Int. Ed.* **45**, 70 (2006).
9. S.-I. Han *et al.*, *Anal. Chem.* **77**, 4008 (2005).
10. M. M. Spence *et al.*, *J. Am. Chem. Soc.* **126**, 15287 (2004).
11. A. Bifone *et al.*, *Proc. Natl. Acad. Sci. U.S.A.* **93**, 12932 (1996).
12. K. M. Ward, A. H. Aletras, R. S. Balaban, *J. Magn. Res.* **143**, 79 (2000).
13. A. A. Maudsley, S. K. Hilal, W. H. Perman, H. E. Simon, *J. Magn. Res.* **51**, 147 (1983).
14. N. Goffeney, J. W. M. Bulte, J. Duyn, L. H. Bryant, P. C. M. van Zijl, *J. Am. Chem. Soc.* **123**, 8628 (2001).
15. K. Knagge, J. Prange, D. Raftery, *Chem. Phys. Lett.* **397**, 11 (2004).
16. J. L. Mynar, T. J. Lowery, D. E. Wemmer, A. Pines, J. M. Frechet, *J. Am. Chem. Soc.* **128**, 6334 (2006).
17. B. M. Goodson *et al.*, *Proc. Natl. Acad. Sci. U.S.A.* **94**, 14725 (1997).
18. G. Huber *et al.*, *J. Am. Chem. Soc.* **128**, 6239 (2006).
19. J. P. Mugler *et al.*, *Magn. Res. Med.* **37**, 809 (1997).
20. S. D. Swanson, M. S. Rosen, K. P. Coulter, R. C. Welsh, T. E. Chupp, *Magn. Res. Med.* **42**, 1137 (1999).

21. This work was supported by the Director, Office of Science, Office of Basic Energy Sciences, Materials Sciences and Engineering Division, of the U.S. Department of Energy under contract no. DE-AC03-76SF00098. L.S. acknowledges support from the Deutsche Forschungsgemeinschaft (SCHR 995/1-1) through an Emmy Noether Fellowship. T.J.L. acknowledges the Graduate Research and Education in Adaptive bio-Technology (GREAT) Training Program of the UC Systemwide Biotechnology Research and Education Program (no. 2005-264), and C.H. acknowledges support from the Schweizerischer Nationalfonds through a postdoctoral fellowship.

Supporting Online Material

www.sciencemag.org/cgi/content/full/314/5798/446/DC1
Materials and Methods
Fig. S1
References

28 June 2006; accepted 29 August 2006
10.1126/science.1131847

Wetland Sedimentation from Hurricanes Katrina and Rita

R. Eugene Turner,[1,2*] Joseph J. Baustian,[1,2] Erick M. Swenson,[1,2] Jennifer S. Spicer[2]

More than 131 × 10^6 metric tons (MT) of inorganic sediments accumulated in coastal wetlands when Hurricanes Katrina and Rita crossed the Louisiana coast in 2005, plus another 281 × 10^6 MT when accumulation was prorated for open water area. The annualized combined amount of inorganic sediments per hurricane equals (i) 12% of the Mississippi River's suspended load, (ii) 5.5 times the inorganic load delivered by overbank flooding before flood protection levees were constructed, and (iii) 227 times the amount introduced by a river diversion built for wetland restoration. The accumulation from hurricanes is sufficient to account for all the inorganic sediments in healthy saltmarsh wetlands.

Inorganic sediments accumulating in coastal wetlands may be delivered from inland sources via (i) unconstrained overbank flooding, (ii) explosive releases through unintentional breaks in constructed levees, and (iii) river diversions. They may also arrive from offshore during tidal inundation or storm events. It is important to know the quantities delivered by each pathway to understand how inorganic sediments contribute to wetland stability and to spend wetland restoration funds effectively. Here we estimate the amount of inorganic sediments deposited on wetlands of the microtidal Louisiana coast during Hurricanes Katrina and Rita.

Hurricanes Katrina and Rita passed through the Louisiana (LA) coast on 29 August and 24 September, 2005, respectively, leaving behind a devastated urban and rural landscape. Massive amounts of water, salt, and sediments were redistributed across the coastal zone within a few hours as a storm surge of up to 5 m propagated in a northerly direction at the coastline south of New Orleans, LA (Katrina), and near Sabine Pass, Texas (TX) (Rita), inundating coastal wetlands in the region. A thick deposit of mud remained in these coastal wetlands after the storm waters receded (Fig. 1). We used this post-storm remnant to learn about how coastal systems work.

The loss of LA's coastal wetlands peaked between 1955 and 1978 at 11,114 ha year^{-1} (*1*) and declined to 2591 ha year^{-1} from 1990 to 2000 (*2*). Coastal wetlands, barrier islands, and shallow waters are thought to provide some protection from hurricanes, by increasing resistance to storm surge propagation and by lowering hurricane storm surge height (*3*). Restoring LA's wetlands has become a political priority, in part because of this perceived wetland/storm surge connection. A major part of LA's restoration effort is to divert part of the Mississippi River into wetlands, and at considerable cost [ref. (*S1*) in supporting online material (SOM)]. Widely adopted assumptions supporting this

[1]Coastal Ecology Institute, [2]Department of Oceanography and Coastal Sciences, Louisiana State University, Baton Rouge, LA 70803, USA.
*To whom correspondence should be addressed. E-mail: euturne@lsu.edu

- **Rainfall responsible for ice-sheet break-up . . .**

  Storms in the tropics and Northern Hemisphere create transoceanic waves linked to the Antarctic ice sheet calving and break-up (MacAyeal, GRL, 2006)

- **Rainfall responsible for triggering earthquake activity . . .**

  Rainfall creates spatio-temporal changes in pore pressure which alters the strength of faults triggering earthquakes (Hainzl et al., GRL, 2006)

- **Rainfall responsible for the Mississippi Delta subsidence . . .**

  (Turner et al., Science, 2006)